*Progress In Electromagnetics Research M, Vol. 59, 171–180, 2017*

# A Low Cost Instantaneous Frequency Measurement System

**Hossam Badran*** **and Mohammad Deeb**

**Abstract**—A new low cost method for implementing an Instantaneous Frequency Measurement (IFM) system is presented in this paper. The proposed method is based on dividing the incoming RF signal into four signals and filtering each one by an appropriate band-pass filter. The frequency is then estimated from the power level of the filtered signals. A closed form for the Standard Deviation (STD) and the bias of the frequency estimator is derived. A design example for an IFM system with a working frequency band of 2 to 4 GHz is presented with simulated and measured results. The design is implemented on a commercial FR4 (DE104) substrate using printed circuit board technology. Experiments in a laboratory show a maximum error of about 15 MHz in estimating the frequency value.

## 1. INTRODUCTION

Instantaneous Frequency Measurement (IFM) systems are an important part of many Electronic Warfare (EW) and electronic intelligence (ELINT) systems. Their role is to determine the carrier frequency of the incoming RF signal over a wide band of frequencies [1, 2]. A conventional IFM system divides the incoming signal into two signals and delays one of them with respect to the other using a delay line with a specified length, then the phase difference between the delayed and non-delayed signal is measured and utilized to extract the frequency value. The phase difference is measured using a phase discriminator, which is most often implemented using power dividers hybrid couplers, and square law detectors [3]. To obtain high accuracy in measuring the frequency, the IFM system components must be carefully designed and fabricated. A very good matching and isolation between the components is required, and the sensitivity of the detectors must be matched very closely. In addition, the delay line loss must be compensated by an equal loss in the direct path [4]. To meet these requirements, an advanced fabrication technology is needed which increases the cost.

Some simpler and lower cost methods but with poor accuracy were presented, by using coplanar strips (CPS) delay-line and multiple band-stop filters [5–7].

In this paper, a new simple and low cost method for implementing an IFM system is presented. The block diagram of the proposed system is shown in Figure 1. It consists of a limiting amplifier 4-way power divider, four band-pass filters (BPF), four logarithmic detectors, four analog to digital converters (ADCs) and a processing unit. The path from each output port of the power divider through the connected band-pass filter, logarithmic detector, and the ADC forms a so called channel.

The RF signal at the system input is amplified by the limiting amplifier to a specified power level of $P_{\text{sat}}$, then it is divided by the power divider to four signals withe qual amplitudes.

Each signal will pass through one of the four band-pass filters where it will be attenuated according to its frequency, thus the frequency of the incoming RF signal can be estimated by measuring the power level of the four filtered signals. The power level of each filtered signal is measured by the logarithmic detector at the filter output. A logarithmic detector produces a voltage proportional to the signal power level at its input. The voltages at the logarithmic detectors outputs are sampled by the ADC's, and the data are fed to the processing unit where the frequency estimation task is performed.

*Received 5 June 2017, Accepted 8 August 2017, Scheduled 17 August 2017*

* Corresponding author: Hossam Badran (hossam.m.badran@gmail.com).
The authors are with the Department of Communication Engineering, Higher Institute of Applied Science and Technology, Damascus, Syria.

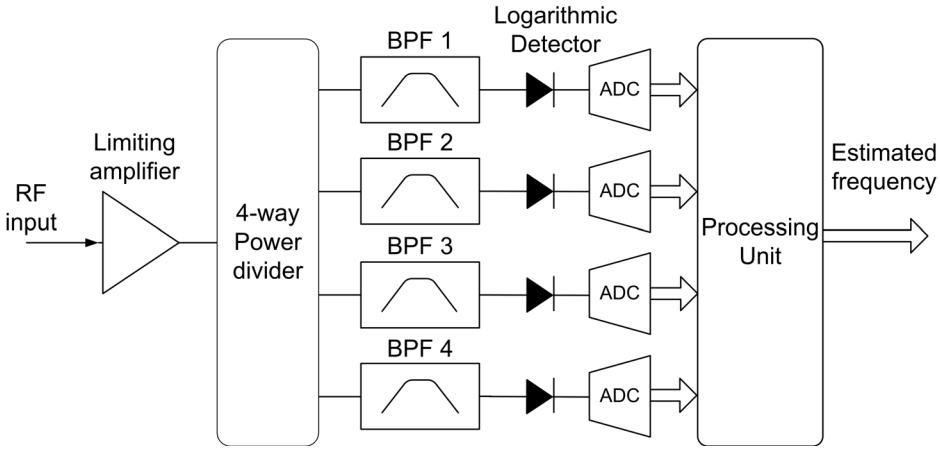


**Figure 1.** Block diagram of the proposed IFM system.

## 2. DETAILED DESCRIPTION OF THE SYSTEM

Assuming an RF signal with unknown frequency $f_0$ present at the system input, the limiting amplifier will amplify and clip this signal to a constant amplitude corresponding to a power level of $P_{\text{sat}}$ [9, 10]. The limiting amplifier used in this work has a nominal output power of $P_{\text{sat}} = 0\,\text{dBm}$.

The signal will then be divided by the 4-way power divider to four signals with equal power level of $P_{\text{sat}} - 6\,\text{dB}$, where 6 dB is the power attenuation caused by the power divider.

Each signal will pass through one channel of the system, where it will be filtered by the corresponding band-pass filter. Designing the band-pass filters is the most important part in the system, the shape of the frequency response of these filters will determine the accuracy of the system. Design considerations of these filters are presented in the next section. Figure 2 shows an example of four band-pass filters that cover the frequency band 2 to 4 GHz.

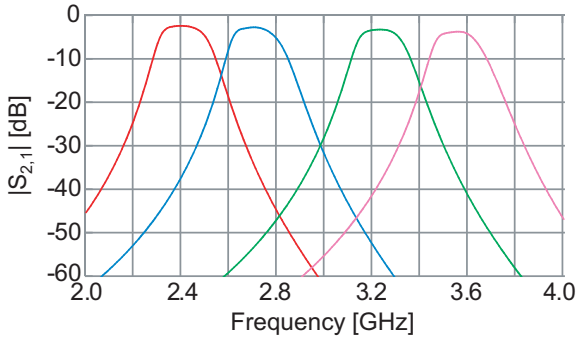


**Figure 2.** Frequency response of a sample band-pass filters.

The power level of the signal at each filter output is:

$$P_{BPF\_k} = P_{\text{sat}} - 6 + A_k(f_0), \quad k = 1, \ldots, 4 \tag{1}$$

Here $A_k(f)$ is the frequency response in dB of the band-pass filter in channel number $k$.

The logarithmic detector at each channel will provide a measure of this power.

A logarithmic detector converts the RF signal present at its input to a corresponding decibel-scaled output voltage, given by [8]:

$$V_o = m(P_{\text{in}} - P_{\text{intercept}}) \tag{2}$$

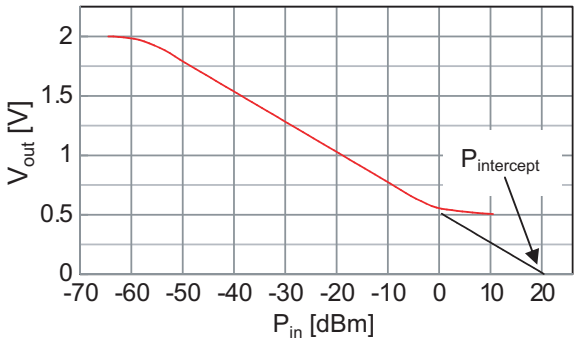


**Figure 3.** Response of the AD8318 logarithmic detector.

Here $P_{\text{in}}$ is the signal power level at the input expressed in dBm, $m$ the slope of the detector's transfer function expressed in V/dB, and $P_{\text{intercept}}$ the intercept point. Equation (2) is valid over a specified dynamic interval from $P_{\text{det-min}}$ to $P_{\text{det-max}}$. Figure 3 shows the output voltage of a sample logarithmic detector, it has a slope of $m = -25\,\text{mV/dB}$, $P_{\text{intercept}} = 20\,\text{dBm}$, and a dynamic interval from $-55$ to $-5\,\text{dBm}$.

Inserting Equation (1) into Equation (2), gives the output voltage of each logarithmic detector that is:

$$V_{ok} = m\left(P_{\text{sat}} - 6\,\text{dB} + A_k(f_0) - P_{\text{intercept}}\right) \triangleq G_k(f_0), \quad k = 1, \ldots, 4 \tag{3}$$

The function $G_k(f)$ is called the transfer function of channel number $k$, which is the voltage at the logarithmic detector output as a function of the input signal frequency.

## 3. DESIGNING THE BAND-PASS FILTERS

As previously mentioned, the shape of the frequency response of the band-pass filters will determine the accuracy of the system. Thus, designing these filters must take into account some considerations.

Also it was mentioned that the signal power level at the logarithmic detector input must be higher than $P_{\text{det-min}}$, so that the signal can be detected and properly measured by the logarithmic detector, i.e.,

$$P_{\text{sat}} - 6\,\text{dB} + A_k(f) \geq P_{\text{det-min}}, \quad \text{or}, \quad A_k(f) \geq P_{\text{det-min}} + 6\,\text{dB} - P_{\text{sat}} \tag{4}$$

Equation (4) shows that the usable part of the frequency response of the filter is the part that has an amplitude higher than $P_{\text{det-min}} + 6\,\text{dB} - P_{\text{sat}}$. This imposes the first constraint on designing the band-pass filters, that is: the usable part of the frequency response of the four filters must cover the required frequency band of the system.

The second constraint comes from the fact that a filter with a sharper frequency response produces more accurate estimation of the frequency (as it will be shown in Section 5); consequently, the filter pass-band — the flat part of its frequency response — doesn't serve in the estimation process. Thus, the flat part of the frequency response of each filter must overlap the frequency response of an adjacent filter.

As long as these two conditions are met, the degree of the filters can be increased to get sharper frequency response, and thus more accurate estimation of the frequency.

Note that increasing the degree of filters will increase the time delay for the output signal to reach its steady state, which will increase the response time of the system. This time delay is better measured by simulation for the filters integrated with the power divider. For the designed system, ADS software is used to measure the delay time from the power divider input to the filters outputs, and simulation shows that the signals at the filters output will reach their steady state after a maximum delay of 25 ns.

Also, it must be mentioned that any number of filters can be used to increase the system accuracy, but this will increase the complexity of the system. In this design, we choose to use four filters to minimize the system complexity.

## 4. TRANSFER FUNCTIONS OF THE SYSTEM AND DATA MODEL

Equation (3) gives the voltages at the logarithmic detectors outputs, where $G_k(f)$ is the transfer function of channel number $k$.

To be able to estimate the frequency $f_0$ from the voltages $V_{o1}, \ldots, V_{o4}$, the transfer function of each channel must be known. To do that, the transfer functions $G_k(f)$'s are measured at a laboratory. Measuring of $G_k$'s is performed by applying a reference signal with known frequency $f_m$ to the system input and measuring the voltages $V_{o1}, \ldots, V_{o4}$ at the logarithmic detectors outputs. The measured voltages are stored into four vectors $G_1, \ldots, G_4$. Then the reference signal frequency $f_m$ is changed by fine steps to scan the frequency band $W$ of the system.

Determining the transfer functions of the system by measurements rather than using mathematical model is more beneficial because measurements contain non-ideal (but systematic) behavior of the system components, such as:

- The variation of the nominal value of the limiting amplifier output power $P_{\text{sat}}$ with frequency.
- The amplitude imbalance at the power divider output ports.
- The variation of the logarithmic detector characteristics (i.e., the slop $m$ and $P_{\text{intercept}}$) with frequency.

After the transfer functions of the system have been measured, the voltages at the logarithmic detectors outputs can be expressed using these transfer functions as:

$$V_{ok} = G_k(f_0) + n_k, \quad k = 1, \ldots, 4 \tag{5}$$

Here $n_k$ is the noise voltage at the output of the logarithmic detector in channel number $k$. These noises are assumed to be uncorrelated with zero mean and variance $\sigma^2$.

The output power level of the limiting amplifier may drift from its nominal value $P_{\text{sat}}$. This drift occurs because of temperature changes. It is distributed equally between all channels, and show up as a voltage drift $e_0$ at the output of the four logarithmic detectors.

Temperature changes also have effect on the output voltage of the logarithmic detectors that will be subjected to small drifts $e_1, e_2, e_3, e_4$.

Taking these voltage drifts into account, Equation (5) becomes:

$$V_{ok} = G_k(f_0) + e_0 + e_k + n_k, \quad k = 1, \ldots, 4 \tag{6}$$

These voltage drifts are caused by temperature changes, so they have a slow variation nature and can be considered fixed within short time interval, or within the time of acquiring samples. The voltages $V_{o1}, \ldots, V_{o4}$ are sampled by the ADC at each channel. For pulsed RF signals, the sampling is performed only within the pulse duration.The acquired samples are:

$$\begin{aligned} Z_1[i] &= G_1(f_0) + e_0 + e_1 + n_1[i] \\ Z_2[i] &= G_2(f_0) + e_0 + e_2 + n_2[i] \\ Z_3[i] &= G_3(f_0) + e_0 + e_3 + n_3[i] \\ Z_4[i] &= G_4(f_0) + e_0 + e_4 + n_4[i], \quad i = 1, \ldots, N \end{aligned} \tag{7}$$

Here $N$ is the number of acquired samples.

The previous equations represent the data model, and the samples $Z_1[i], \ldots, Z_4[i]$ are fed to the processing unit where an estimation algorithm is performed to estimate the frequency value $f_0$.

## 5. ESTIMATING THE FREQUENCY

To estimate the frequency value $f_0$ from the samples $Z_1[i], \ldots, Z_4[i]$, the Least Square (LS) estimator is used, where the estimated value $\hat{f}_0$ of frequency is the value that minimizes the function $J$ in (8):

$$\begin{aligned} J(f) &= \sum_{i=1}^{N} (Z_1[i] - G_1(f))^2 + (Z_2[i] - G_2(f))^2 + (Z_3[i] - G_3(f))^2 + (Z_4[i] - G_4(f))^2 \\ \hat{f}_0 &= \min_f (J(f)) \end{aligned} \tag{8}$$

Taking into account that the transfer functions $G_1, \ldots, G_4$ are stored as numeric values, minimization of $J$ is performed numerically

The performance of the LS frequency estimator is evaluated in Appendix A. the standard deviation (STD) of this estimator is given by:

$$\mathrm{STD}(\hat{f}_0) \approx \sqrt{\frac{\sigma^2/N}{G_1'^2(f_0) + G_2'^2(f_0) + G_3'^2(f_0) + G_4'^2(f_0)}} \tag{9}$$

and the bias is given by:

$$\begin{aligned} \mathrm{bias}(\hat{f}_0) &= E\left(\hat{f}_0 - f_0\right) \\ &\approx \frac{e_1 G_1'(f_0) + e_2 G_2'(f_0) + e_3 G_3'(f_0) + e_4 G_4'(f_0) + e_0\left[G_1'(f_0) + G_2'(f_0) + G_3'(f_0) + G_4'(f_0)\right]}{G_1'^2(f_0) + G_2'^2(f_0) + G_3'^2(f_0) + G_4'^2(f_0)} \end{aligned} \tag{10}$$

where:

$$G_k'(f) = \frac{\partial G_k(f)}{\partial f}, \quad k = 1, \ldots, 4 \tag{11}$$

If the voltage drifts are within the interval from $-e_{\max}$ to $e_{\max}$, then, the maximum absolute value of the bias is given by (see Appendix A):

$$\max\_\mathrm{bias}(\hat{f}_0) = e_{\max} \frac{|G_1'(f_0)| + |G_2'(f_0)| + |G_3'(f_0)| + |G_4'(f_0)| + |G_1'(f_0) + G_2'(f_0) + G_3'(f_0) + G_4'(f_0)|}{G_1'^2(f_0) + G_2'^2(f_0) + G_3'^2(f_0) + G_4'^2(f_0)} \tag{12}$$

We note that the bias of the estimator depends on the voltage drifts $e_0, \ldots, e_4$, and these voltage drifts have a slow variation over time (as mentioned in Section 4), thus performing multiple measurements for the same signal within a short time interval cannot improve the bias, but it can decrease the STD of the estimator. However, we will see that the estimator bias is much higher than its STD.Thus, performing multiple measurements for the same signal can't effectively improve the estimation.

Equations (9) and (10) show that the STD and the bias of the frequency estimator depend on the frequency value $f_0$ and are inversely proportional to $G_k'$. This means that a system with sharper transfer functions produces a more accurate frequency estimate.

Note that in a well designed system, the transfer function $G_k$ has nearly the same shape of the frequency response of the band-pass filter number $k$. This makes Equations (9) and (12) to be of great importance when designing the bandpass filters. The filters are designed and simulated using software design tools, while Equations (9) and (12) provide a prior knowledge about the resulting estimator accuracy, thus the frequency response of the filters can be adjusted in order to minimize the variance and the bias of the estimator.

Calculating the LS estimator needs to compute the function $J(f)$ in Equation (8) and then, find its minimum. This will need some time to be done depending on the platform used for performing the calculations. Some notes can be made to decrease the calculations time.

Noting that the function $J(f)$ can be written as

$$\begin{aligned} J(f) \;=\; & \sum_{i=1}^{N}\left(Z_1^2[i]\right) + NG_1^2(f) - 2G_1(f)\sum_{i=1}^{N}\left(Z_1[i]\right) \;+\; \sum_{i=1}^{N}\left(Z_2^2[i]\right) + NG_2^2(f) \\ & -2G_2(f)\sum_{i=1}^{N}\left(Z_2[i]\right) + \sum_{i=1}^{N}\left(Z_3^2[i]\right) + NG_3^2(f) - 2G_3(f)\sum_{i=1}^{N}\left(Z_3[i]\right) \\ & + \sum_{i=1}^{N}\left(Z_4^2[i]\right) + NG_4^2(f) - 2G_4(f)\sum_{i=1}^{N}\left(Z_4[i]\right). \end{aligned}$$

The quantities $\sum_{i=1}^{N}(Z_k[i])$ and $\sum_{i=1}^{N}(Z_k^2[i])$ can be computed during sampling process, and the quantity $G_k^2(f)$ is pre-computed and stored in a memory. Once the sampling process is finished, the quantities $\sum_{i=1}^{N}(Z_k[i])$ and $\sum_{i=1}^{N}(Z_k^2[i])$ will be ready, and the computation of function $J(f)$ can start.

The use of field programmable gates array (FPGA) to perform calculations is reasonable here, because the calculations can be performed in parallel at different points of frequencies.

Using pipelining technique, the calculation of $J(f)$ at each frequency point can be performed during one clock (if 100 MHz clock is used, then the clock period is 10 ns), but this requires the use of 8 multipliers, 11 adders, and one comparators, working simultaneously.

Thus using 80 multipliers, 110 adders, and 10 comparators, make it possible to calculate $J(f)$ at 10 points of frequency during one clock cycle.

In the presented 2 to 4 GHz system, the transfer functions are measured at a frequency step of 2 MHz, thus the number of the frequency points is $M = 1000$. So we need 100 clock cycles to compute $J(f)$, which corresponds to 1 μs.

The proposed number of arithmetic elements are very usual in a medium density FPGA.

Using high density FPGA circuit can offer more arithmetic elements, and can reduce the calculations time to a few hundreds of nanoseconds.

## 6. DESIGN EXAMPLE AND EXPERIMENTAL RESULTS

An IFM system with working frequency band $W$ from 2 to 4 GHz is designed and implemented. The microwave circuit of the system is shown in Figure 4, and it consists of a 4-way power divider (1 : 4 PD and four band-pass filters (BPF1, BPF2, BPF3, BPF4), and port $P_1$ is the input port, and ports $P_2, P_3, P_4, P_5$ are the output ports.

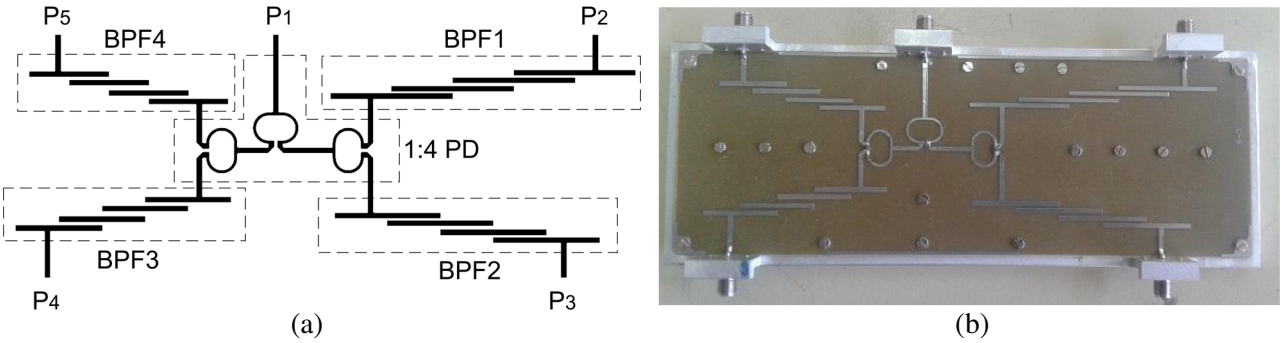


**Figure 4.** (a) Layout of the microwave circuit. (b) Photograph of the fabricated microwave circuit.

The 4-way power divider is designed using three identical 2-way Wilkinson power dividers with one section, and each 2-way power divider is designed at center frequency of 3 GHz. Figure 5(a) shows the 4-way power divider with physical dimensions.

The lengths of the transmission lines between the first 2-way divider and the other two, and between the power divider and the band-pass filters are $a_1, a_2, a_3, a_4, a_5, a_6$. These lengths are adjusted by simulation to achieve the desired frequency response from input to output ports, i.e., $|S_{21}|$, $|S_{31}|$, $|S_{41}|$, $|S_{51}|$.

The physical dimensions of the power divider are shown in Table 1 (in mm).

**Table 1.** Physical dimensions (in mm) of the fabricated 4-way power divider.

| Dimension | | Dimension | | Dimension | |
|---|---|---|---|---|---|
| $W_1$ | 0.808 | $d_3$ | 1.213 | $a_3$ | 12.5 |
| $W_2$ | 1.516 | $r$ | 4 | $a_4$ | 15.5 |
| $d_1$ | 4.064 | $a_1$ | 14 | $a_5$ | 10.95 |
| $d_2$ | 1 | $a_2$ | 8.75 | $a_6$ | 10.95 |

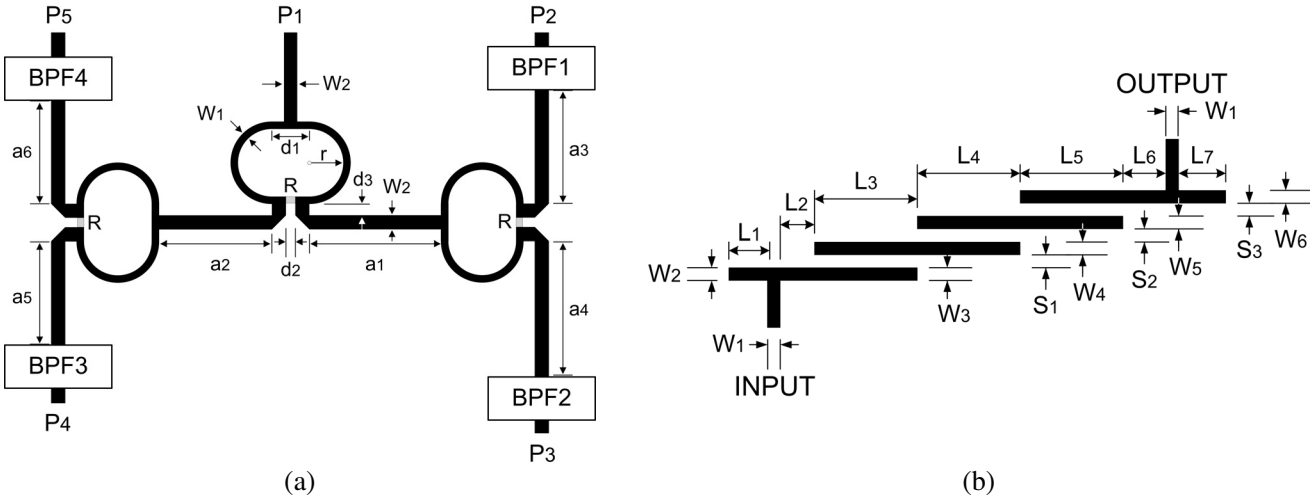


**Figure 5.** (a) The designed 4-way power divider. (b) Prototype of the designed band-pass filters.

The value of the three resistors $R$ is 100 Ω.

Four 4th order Butterworth band-pass filters are designed using coupled lines with tapped input and output topology. The center frequencies of these filters are: 2.39, 2.75, 3.36, 3.64 GHz, and the −3 dB band width are: 260, 270, 230, 280 MHz, respectively. The prototype of these filers is shown in Figure 5(b).

The physical dimensions of these filters are shown in Table 2 (in mm).

The circuit is implemented on an FR4 (DE104) substrate with a dielectric constant of 4.2, loss tangent of 0.02, and thickness of 0.8 mm. Figure 6(a) shows the simulated and measured insertion losses from the input to the output ports, i.e., $|S_{21}|$, $|S_{31}|$, $|S_{41}|$, and $|S_{51}|$. The simulation is carried out using the ADS EM simulator software. As shown, there is a good agreement between the simulated and measured values. There is high ripple in the measured values at an amplitude level below −50 dB. This ripple is caused by cables and SMA connectors and will not affect the estimation process because the logarithmic detectors will not respond to signals with such a low amplitude.

**Table 2.** Physical dimensions (in mm) of the designed band-pass filters.

| | BPF1 | BPF2 | BPF3 | BPF4 |
|---|---|---|---|---|
| $L_1$ | 10.62 | 9.42 | 8.26 | 7.4 |
| $L_2$ | 5.11 | 3.99 | 2.4 | 2.32 |
| $L_3$ | 17.5 | 15.11 | 12.26 | 11.33 |
| $L_4$ | 17.38 | 15.02 | 12.22 | 11.29 |
| $L_5$ | 17.5 | 15.11 | 12.26 | 11.33 |
| $L_6$ | 4.99 | 4.24 | 2.57 | 2.44 |
| $L_7$ | 10.62 | 9.42 | 8.27 | 7.4 |
| $W_1$ | 1.52 | 1.52 | 1.52 | 1.52 |

| | BPF1 | BPF2 | BPF3 | BPF4 |
|---|---|---|---|---|
| $W_2$ | 1.53 | 1.53 | 1.53 | 1.53 |
| $W_3$ | 1.49 | 1.49 | 1.51 | 1.51 |
| $W_4$ | 1.49 | 1.49 | 1.51 | 1.51 |
| $W_5$ | 1.53 | 1.53 | 1.53 | 1.53 |
| $S_1$ | 0.57 | 0.67 | 1.02 | 0.92 |
| $S_2$ | 0.96 | 1.08 | 1.51 | 1.38 |
| $S_3$ | 0.57 | 0.67 | 1.02 | 0.92 |

A limiting amplifier with $P_{\text{sat}} = 0$ dBm is placed at the system input, and the AD8318 logarithmic detector from ANALOG DEVICES is placed at the output of each filter. The typical values of slope and $P_{\text{intercept}}$ of this logarithmic detector are stated as −24.4 mV/dB and from 19.6 to 25 dBm respectively within the interval from 1.9 to 5.8 GHz. The dynamic range of the AD8318 logarithmic detector is from −55 to −5 dBm.

The transfer functions of the system have been measured at a laboratory several times at different

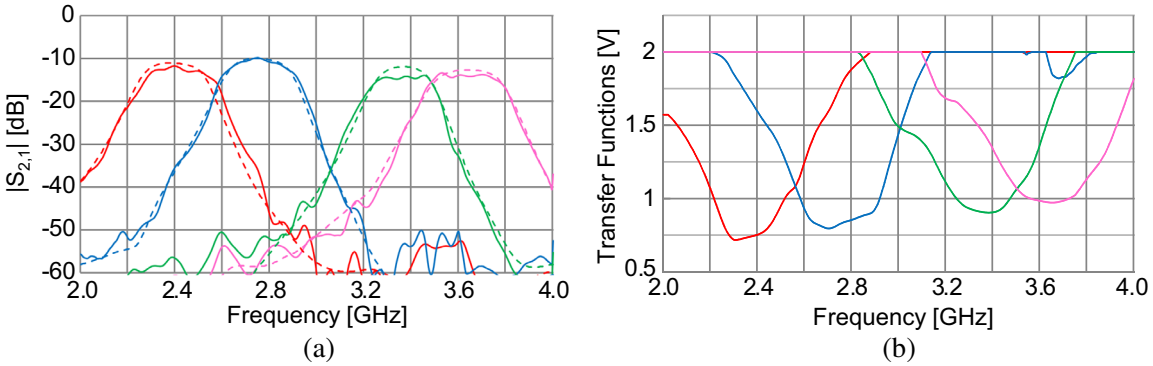


**Figure 6.** (a) EM simulated (dot), and measured (solid) values of $|S_{21}|$, $|S_{31}|$, $|S_{41}|$, $|S_{51}|$. (b) Measured transfer functions of the system, $G_1$, $G_2$, $G_3$, and $G_4$.

degrees of temperature and averaged. The measured transfer functions are clipped manually to a maximum value of 2 V. Figure 6(b) shows the measured transfer functions.

The transfer functions have nearly the same shape of the measured insertion loss shown in Figure 6(a) but with up-down flipping. The difference between the two shapes is due to the changes in logarithmic detectors response with frequency and the non-perfect matching of the detectors.

After measuring the transfer functions of the designed system, the frequency of the incoming signal can be estimated using the LS estimator. The performance of the frequency estimator is evaluated using Monte-Carlo simulation, the following values are assumed in simulation:

- The variance of noise at logarithmic detectors output is $\sigma^2 = (10\,\text{mV})^2$.
- The number of acquired samples from each channel is $N = 25$ samples.
- The voltage drifts $e_0, \ldots, e_4$ are uniformly distributed within the interval from $-10$ to 10 mV, and they are fixed in each simulation run.

Simulation results show that the STD of the frequency estimator is less than 1.3 MHz, and it is very close to the approximated value computed from Equation (9), as shown in Figure 7.

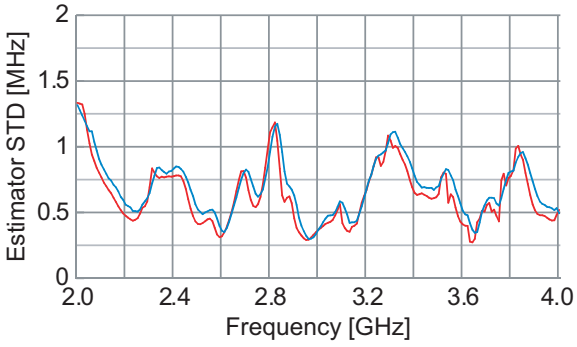


**Figure 7.** Approximated (red), and simulated (blue) STD of the frequency estimator.

Also, the maximum absolute bias of the frequency estimator is less than 15 MHz, and it is very close to the approximated value computed from Equation (12), as shown in Figure 8.

The maximum absolute value of the bias is relatively high and attains 15 MHz at some frequencies. In practice, the maximum bias is reached only for certain values of the voltage drifts. So in order to see how the bias is distributed between its maximum and minimum values, the 90% confidence interval is calculated by simulation. Assuming that the voltage drifts are uniformly distributed over the interval from $-10$ to 10 mV, the 90% confidence interval of the bias is less than 10 MHz, as shown in Figure 8.

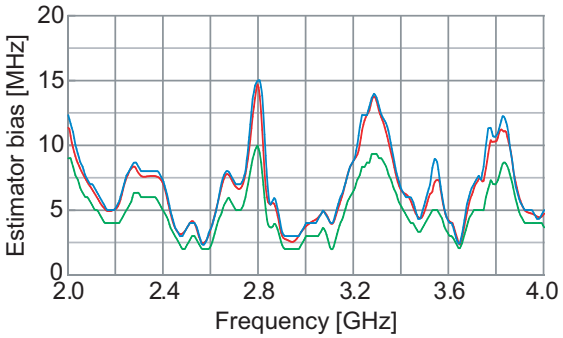


**Figure 8.** Approximated (red) and simulated (blue) maximum absolute bias of the frequency estimator. And the 90% confidence interval of the bias (green).

## 7. CONCLUSION

In this paper, a new low cost method for implementing an IFM system is presented. In this method, a set of four band-pass filters are used to estimate the frequency of the incoming RF signal. The accuracy of this method is analyzed and described by closed forms. A design example with working frequency band of 2 to 4 GHz is presented with simulated and measured results. For practical values of noise and measurements drifts, the designed system shows an accuracy of less than 10 MHz over most of the working frequency band and less than 15 MHz over the total working frequency band.

## APPENDIX A.

The Least Square (LS) estimator is used to compute an estimated value $\hat{f}_0$ for $f_0$. The variance and bias of this estimator will be evaluated in this appendix.

The estimated value $\hat{f}_0$ is the value that minimize the function $J(f)$ in Eq. (A1).

$$J(f) = \sum_{i=1}^{N} (Z_1[i] - G_1(f))^2 + (Z_2[i] - G_2(f))^2 + (Z_3[i] - G_3(f))^2 + (Z_4[i] - G_4(f))^2 \tag{A1}$$

Instead of minimizing $J(f)$, the LS estimator can be found as the solution of Equation (A2)

$$\begin{aligned} \left.\frac{\partial J(f)}{\partial f}\right|_{f=\hat{f}_0} = 0 = -2\sum_{i=1}^{N} \Big\{ &\left(Z_1[i] - G_1(\hat{f}_0)\right) G_1'(\hat{f}_0) + \left(Z_2[i] - G_2(\hat{f}_0)\right) G_2'(\hat{f}_0) \\ &+ \left(Z_3[i] - G_3(\hat{f}_0)\right) G_3'(\hat{f}_0) + \left(Z_4[i] - G_4(\hat{f}_0)\right) G_4'(\hat{f}_0) \Big\} \end{aligned} \tag{A2}$$

Where

$$G_k'(f) = \frac{\partial G_k(f)}{\partial f}, \quad k = 1, \ldots, 4 \tag{A3}$$

And this solves the equation:

$$\left(\bar{Z}_1 - G_1(\hat{f}_0)\right) G_1'(\hat{f}_0) + \left(\bar{Z}_2 - G_2(\hat{f}_0)\right) G_2'(\hat{f}_0) + \left(\bar{Z}_3 - G_3(\hat{f}_0)\right) G_3'(\hat{f}_0) + \left(\bar{Z}_4 - G_4(\hat{f}_0)\right) G_4'(\hat{f}_0) = 0 \tag{A4}$$

where $\bar{Z}_k$ is computed from Eq. (7) as:

$$\bar{Z}_k = \frac{1}{N}\sum_{i=1}^{N} Z_k[i] = G_k(f_0) + e_0 + e_k + \frac{1}{N}\sum_{i=1}^{N} n_k[i] = G_k(f_0) + e_0 + e_k + \bar{n}_k \tag{A5}$$

Replacing Eqs. (A5) into (A4) gives

$$\begin{aligned} &\left(G_1(f_0) + e_0 + e_1 + \bar{n}_1 - G_1(\hat{f}_0)\right) G_1'(\hat{f}_0) + \left(G_2(f_0) + e_0 + e_2 + \bar{n}_2 - G_2(\hat{f}_0)\right) G_2'(\hat{f}_0) + \\ &\left(G_3(f_0) + e_0 + e_3 + \bar{n}_3 - G_3(\hat{f}_0)\right) G_3'(\hat{f}_0) + \left(G_4(f_0) + e_0 + e_4 + \bar{n}_4 - G_4(\hat{f}_0)\right) G_4'(\hat{f}_0) = 0 \end{aligned} \tag{A6}$$

Note that the transfer functions of the system do not suffer from fast variations and can be approximated by a line in the vicinity of $f$, thus

$$G_k(f_0) - G_k(\hat{f}_0) \approx (f_0 - \hat{f}_0)G'_k(f_0) \tag{A7}$$

Replacing Eq. (A7) into Eq. (A6) and rearranging gives

$$\hat{f}_0 - f_0 \approx \frac{1}{A}\left[(e_0+e_1+\bar{n}_1)\,G'_1(f_0)+(e_0+e_2+\bar{n}_2)\,G'_2(f_0)+(e_0+e_3+\bar{n}_3)\,G'_3(f_0)+(e_0+e_4+\bar{n}_4)\,G'_4(f_0)\right] \tag{A8}$$

where:

$$A = G'^2_1(f_0) + G'^2_2(f_0) + G'^2_3(f_0) + G'^2_4(f_0) \tag{A9}$$

Taking the variance of both sides of Eq. (A8) gives the variance of the LS estimator:

$$\mathrm{var}(\hat{f}_0) \approx \frac{\sigma^2/N}{A} \tag{A10}$$

Taking the expectation of both sides of Eq. (A8) gives the bias of the estimator:

$$\begin{aligned}\mathrm{bias}(\hat{f}_0) = E\left(\hat{f}_0 - f_0\right) &\approx \frac{1}{A}\left[(e_0+e_1)\,G'_1(f_0)+(e_0+e_2)\,G'_2(f_0)+(e_0+e_3)\,G'_3(f_0)+(e_0+e_4)\,G'_4(f_0)\right] \\ &\approx \frac{1}{A}\left[e_1G'_1(f_0)+e_2G'_2(f_0)+e_3G'_3(f_0)+e_4G'_4(f_0)+e_0\left(G'_1(f_0)+G'_2(f_0)+G'_3(f_0)+G'_4(f_0)\right)\right]\end{aligned} \tag{A11}$$

Assuming that the voltage drifts $e_0, e_1, e_2, e_3, e_4$ are within the interval $[-e_{\max},\ e_{\max}]$, the maximum absolute bias is

$$\mathrm{max\_bias}(\hat{f}_0) \approx \frac{e_{\max}}{A}\left|G'_1(f_0)\right|+\left|G'_2(f_0)\right|+\left|G'_3(f_0)\right|+\left|G'_4(f_0)\right|+\left|G'_1(f_0)+G'_2(f_0)+G'_3(f_0)+G'_{41}(f_0)\right| \tag{A12}$$

## REFERENCES


1. Liang, G. C., C. F. Shien, R. S. Withers, B. F. Cole, M. A. Johansson, and L. P. Suppan, "Superconductive digital instantaneous frequency measurement subsystem," *IEEE Trans. Microw. Theory Tech.*, Vol. 41, No. 12, 2368–2375, Dec. 1993.
2. Gruchala, H. and M. Czyzewski, "The instantaneous frequency measurement receiver in the complex electromagnetic environment," *15th Int. Microw. Radar Wireless Commun. Conf.*, Vol. 1, 17–19, 155–158, May 2004.
3. East, P. W., "Design techniques and performance of digital IFM," *Proc. IEE*, Pt. F, 154–163, 129, 1982.
4. East, P. W., "Fifty years of instantaneous frequency measurement," *IET Radar, Sonar & Navigation*, Vol. 6, No. 2, 2012.
5. Biehl, M., A. Vogt, R. Herwig, M. Neuhaus, E. Crocoll, R. Lochschmied, T. Scherer, and W. Jutzi, "A 4 bit instantaneous frequency meter at 10 GHz with coplanar YBCO delay lines," *IEEE Applied Superconductivity*, Vol. 5, No. 2, 1995.
6. De Oliveira, B. G. M., F. R. Le Silva, M. T. de Melo, and L. R. G. S. L. Novo, "A new coplanar interferometer for a 5–6 GHz instantaneous frequency measurement system," *IEEE Microwave and Optoelectronic Conference*, 2009.
7. De Souza, M. F. A., F. R. Le Silva, M. T. de Melo, and L. R .G. S. L. Novo, "Discriminator for instantaneous frequency measurement subsystem based on open-loop resonators" *IEEE Microwave Theory and Techniques*, Vol. 57, No. 9, Sep. 2009.
8. Khramov, K., "The study of statistical characteristics of signals at their processing in logarithmic detector," *Second International Scientific-Practical Conference Problems of Infocommunications, Science and Technology*, 2015.
9. Moghe, S. B., S. Consolazio, and H. Fudem, "Electronic warfare II — Receivers," *Gallium Arsenide Applications Handbook*, Vol. 1, 203, 1995.
10. Tsui, J. B., *Microwave Receivers with Electronic Warfare Applications*, 189, SciTech Publishing Inc., 2005.